Broadband Spatially Feedforward Active Noise Control Algorithms Using a Comb Filter

Mingsian R. Bai
E-mail: msbai@mail.nctu.edu.tw

Jienwen Lai

Department of Mechanical Engineering,
National Chiao-Tung University,
1001 Ta-Hsueh Rd., Hsin-Chu 300,
Taiwan, Republic of China

A controller composed of a nonrecursive filter and a recursive filter is used to approximate the ideal controller for a spatially feedforward duct ANC problem. The nonrecursive part represents the dynamics of the transducer, whereas the recursive part is in the form of a comb filter. The parameters of the comb filter are obtained from the impulse response of the controller by using the least-square method. The comb filter is then cascaded with the nonrecursive part implemented as either a fixed filter or an adaptive filter. In the latter approach, two types of LMS-based algorithms are used. The proposed algorithms are implemented on the platform of a digital signal processor. Experimental results showed that the approximated controller attained 17 dB maximal attenuation in the frequency band 200∼600 Hz. [DOI: 10.1115/1.1525003]

1 Introduction

Active control for noise in ducts has provoked much interest in the area of active noise control (ANC) over the past decades [1–4]. In ANC applications to date, feedforward control has been widely used whenever a nonacoustical reference can be obtained. However, when broadband attenuation is of interest, it has been recognized that the *spatially feedforward control* structure depicted in Fig. 1(*a*) is better suited to practical situations in which a nonacoustical reference required by purely feedforward control is unavailable [5–7]. A thorough analysis of the spatially feedforward structure for duct ANC problems was conducted by Bai et al. [5]. In their work, a fixed controller was derived and implemented. The impulse response of the spatially feedforward controller exhibits a periodic pattern with decaying amplitude. It was also shown that the controller could be decomposed into a nonrecursive (finite impulse response, FIR) part and a recursive (infinite impulse response, IIR) part. The former is dependent on transducer properties, while the later is dependent on the duct-medium properties. The advantage of such a decomposition scheme stems from not only physical insights but also simplicity of the resulting filters (instead of a single FIR filter with long taps). In this paper, we shall extend this idea to exploit the simple structure of the IIR part and implement it as a *damped comb filter*. The synthesis of the comb filter is based on a least-square fit of the impulse response. On the other hand, two approaches are also adopted in the realization of the FIR part. The first approach is to implement it as a fixed FIR filter. The second is to update the FIR filter adaptively by using the *filtered-x least-mean-square algorithm* (FXLMS) and the *normalized filtered-x least-mean-square algorithm* (NFXLMS) [4] such that perturbations and uncertainties in the system can be better accommodated. The proposed algorithms are implemented on the platform of a floating-point digital signal processor (DSP). Experimental results indicate that the proposed spatially feedforward ANC system is capable of achieving broadband attenuation of random noise in duct.

The organization of this paper is as follows. Section 1 addresses the ideal controller for spatially feedforward duct ANC system and the synthesis of its IIR part by using a comb filter. Section 2 presents the integration of the controller as well as its reformulation into an adaptive version. Section 3 reports the experimental verification of the proposed system. Section 4 summarizes the current work and future perspective of research.

Contributed by the Technical Committee on Vibration and Sound for publication in the JOURNAL OF VIBRATION AND ACOUSTICS. Manuscript received April 2001; Revised August 2002. Associate Editor: R. Ohayon.

2 Controller Synthesis Using a Comb Filter

2.1 Ideal Controller for Spatially Feedforward Duct ANC. The spatially feedforward ANC structure of a duct and its equivalent circuit are shown in Fig. 1. Based on the concept of acoustic short-circuit, Munjal and Eriksson [8] derived an ideal controller for achieving global noise cancellation downstream the control source in a finite-length duct:

$$C_{ideal} = -\frac{Z_{sa}}{Y_0}\left(\frac{e^{-jkl_i}}{1-e^{-2jkl_i}}\right) = C_{EM}\cdot C_{RP}, \tag{1}$$

where Z_{sa} is the acoustic impedance of the control source, $Y_0 = c/S$ is the characteristic impedance of the duct, c is the sound speed, S is the cross-sectional area of the duct, k is wavenumber, and l_i is the distance between the upstream measurement microphone and the control source. This ideal controller is an infinite-dimensional controller without any modal truncation. In Eq. (1),

$$C_{EM} \equiv -\frac{Z_{sa}}{Y_0} \tag{2}$$

is a function of the finite impedance Z_{sa} which is dependent on only the electro-mechanical parameters of the control source. On the other hand,

$$C_{RP} \equiv \frac{e^{-jkl_i}}{1-e^{-2jkl_i}} \tag{3}$$

is known as the *repetitive controller* [9] which will periodically reproduce an arbitrary input signal of any finite duration. It is not difficult to see that both frequency response and impulse response of the above ideal controller exhibit patterns of periodic peaks. The repetitive peaks in fact result from the acoustic feedback in spatially feedforward structures. For the spatially feedforward ANC structure, the ideal controller is a function independent of the upstream and downstream conditions, which provides portability of the controller among different systems.

It has been shown in [5] that the aforementioned ideal controller can be approximated using the following frequency-domain formula:

$$C_{ideal}(e^{j\omega}) = \frac{-H_0(e^{j\omega})}{H_2(e^{j\omega}) - H_1(e^{j\omega})H_0(e^{j\omega})}, \tag{4}$$

where $H_0(e^{j\omega})$ is the frequency response function between the downstream performance microphone and the upstream measurement microphone, $H_1(e^{j\omega})$ is the frequency response function be-

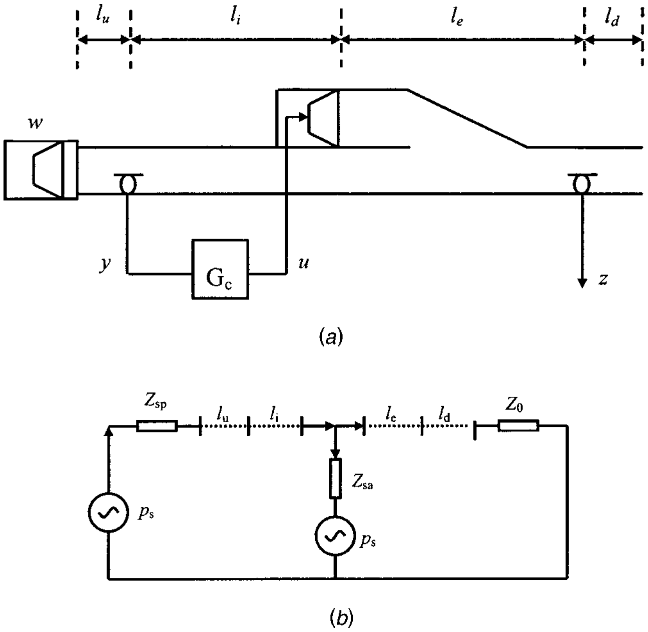

Fig. 1 The spatially feedforward structure of ANC system (*a*) the schematic duct ANC system (*b*) equivalent circuit

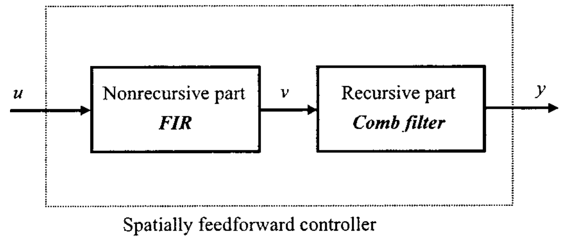

Fig. 2 Block diagram of the fixed spatially feedforward controller composed of a nonrecursive FIR and a recursive comb filter

tween the upstream measurement microphone and the control loudspeaker, and $H_2(e^{j\omega})$ is the frequency response function between the downstream performance microphone and the control loudspeaker. These frequency response functions can be easily measured by a spectral analyzer.

2.2 Approximation of the Repetitive Controller Using a Comb Filter. A direct simplification of ANC design can be gained by exploiting the distinct structure of the ideal controller of Eq. (1). In contrast to conventional FIR implementation, the number of filter coefficients can be substantially reduced by casting the IIR part of the spatially feedforward controller into the form of a damped comb filter.

Referring to the block diagram of Fig. 2, the cascaded filters of Eq. (1) can be discretized into the following transfer function form:

$$H(z)=(b_0+\ldots+b_M z^{-M})\cdot\frac{1}{1-gz^{-N}}. \tag{5}$$

Note that M is the tap length of the FIR part, $(1-gz^{-N})$ corresponds to the discrete-time version of $(1-e^{-2jkl_i})$, sample delay $N=2l_i/cT$, where c is the sound speed and T is the sampling period. The real constant g is introduced as a damping factor which is dependent on the directivity of transducers and the absorptivity of duct wall. The IIR part is in fact a damped comb filter whose simple structure renders a considerable saving in filtering operation:

$$y(k)=g\cdot y(k-N)+u(k) \tag{6}$$

where y and u are output signal and input signal, respectively.

Next, the coefficients $b_0\sim b_M$ in Eq. (5) can be estimated using a procedure similar to room response approximation in audio signal processing [10]. Assume that the controller of Eq. (5) is equivalent to an all-zero filter with coefficients being the impulse response of the filter of Eq. (4)

$$\frac{b_0+\ldots+b_M z^{-M}}{1-gz^{-N}}=\sum_{n=0}^{\infty}h(n)z^{-n} \tag{7}$$

Multiplying both sides of Eq. (7) by the denominator $(1-gz^{-N})$ gives

$$(b_0+\ldots+b_M z^{-M})=\left(\sum_{n=0}^{\infty}h(n)z^{-n}\right)(1-gz^{-N}). \tag{8}$$

Truncating the controller impulse response to K samples and comparing the coefficients of like powers on both sides leads to the following set of linear equations:

$$\begin{bmatrix} b_0\\ b_1\\ \vdots\\ b_M\\ 0\\ \vdots\\ 0\end{bmatrix}=\begin{bmatrix} h_0 & 0 & 0 & \cdots & 0\\ h_1 & h_0 & 0 & \cdots & 0\\ \vdots & \vdots & \vdots & \vdots & \\ h_M & h_{M-1} & h_{M-2} & \cdots & h_{M-N}\\ h_{M+1} & h_M & h_{M-1} & \cdots & h_{M-N+1}\\ \vdots & \vdots & \vdots & & \vdots\\ h_K & h_{K-1} & h_{K-2} & \cdots & h_{K-N}\end{bmatrix}\begin{bmatrix}1\\ 0\\ \vdots\\ -g\end{bmatrix}. \tag{9}$$

In what follows, the coefficients $b_0\ldots b_M$ and the damping factor g in the above equation are determined in two steps. First, the coefficient g of the comb filter is estimated from the exponentially decaying envelope of the measured impulse response. Second, the vector $[1\ 0\ldots g]^T$ is then substituted into Eq. (9) to determine the coefficients $[b_0\ b_1\ldots b_M]^T$. The damping factor g can be estimated by curve-fitting the peaks of the controller impulse response in logarithmic scale with a straight line. From the slope of the straight line, one is able to determine the parameter g. Let the straight line be expressed as

$$\ln h=pt+q, \tag{10}$$

where h is the peak value of impulse response of the controller, t is the corresponding time index, p is the slope of the straight line, and q is the intersection of the line with the vertical axis. Substitution of the measured data yields the following linear system of equations

$$\begin{bmatrix}\ln h_1\\ \vdots\\ \ln h_n\end{bmatrix}=\begin{bmatrix} t_1 & 1\\ t_2 & 1\\ \vdots & \vdots\\ t_n & 1\end{bmatrix}\begin{bmatrix}p\\ q\end{bmatrix}, \tag{11}$$

where n is number of peaks. In matrix notation, Eq. (11) can be written into a more compact form:

$$\mathbf{b}=\mathbf{A}\mathbf{x} \tag{12}$$

The matrix $\mathbf{A}$ is generally over-determined and hence not square. The least square solution of Eq. (12) is

$$\mathbf{x}=\mathbf{A}^{+}\mathbf{b}, \tag{13}$$

where $\mathbf{A}^{+}=(\mathbf{A}^H\mathbf{A})^{-1}\mathbf{A}^H$ is the pseudo inverse of $\mathbf{A}$ [11]. The slope p can be retrieved from the first element of the vector $\mathbf{x}$. In Fig. 3, the peak values of the controller impulse response are plotted along with the fitting straight line $(n=5)$. On the other hand, the parameter g is obtained from

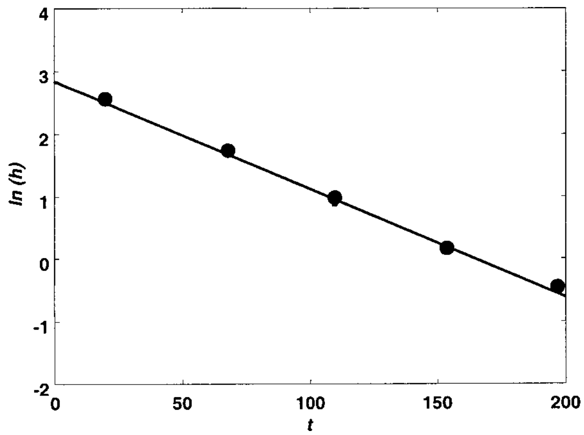

Fig. 3 Curve-fit for the peak values of the impulse response of the spatially feedforward controller using the least-square method

$$g = e^{N \cdot p} \tag{14}$$

In the special case when $M = N$, the FIR coefficients $b_0 \sim b_M$ can simply be calculated using the following formula

$$b_m = h_m, \quad \text{for } m = 0,1, \ldots, M-1$$

$$b_M = h_M - g h_0. \tag{15}$$

In this case, the FIR coefficients except b_M are found to be the replica of the first M samples of the controller impulse response. The damped comb filter hence creates the repetitive and decaying impulse response pattern from these M samples. This technique when applied to the ANC problem in the study gives rise to substantial reduction of computational complexity.

3 Conversion to Adaptive Algorithms

The ANC algorithm for spatially feedforward structure developed in last section is essentially a fixed controller. In practical applications, it may be advantageous to have an adaptive controller so that system uncertainties and perturbations can be better accommodated. To this end, an adaptive filter is incorporated into the controller in place of the aforementioned fixed controller.

3.1 Review of Two LMS-based Algorithms. A brief review of two LMS-based algorithms widely used in ANC area shall be given. First, we review the FXLMS algorithm [4]. The error signal is expressed as

$$e(n) = d(n) - y'(n) = d(n) - s(n) * y(n)$$

$$= d(n) - s(n) * [\mathbf{w}^T(n)\mathbf{x}(n)], \tag{16}$$

where $s(n)$ is the impulse response of secondary path $S(z)$ at the time n, $*$ denotes linear convolution, $\mathbf{w}(n) = [w_0(n) w_1(n) \ldots \ldots w_{L-1}(n)]^T$ is the coefficient vector of the FIR filter $W(z)$, $\mathbf{x}(n) = [x(n) x(n-1) \ldots \ldots x(n-L+1)]^T$ is the reference signal vector, and L is the order of filter $W(z)$. The FXLMS method minimizes the instantaneous squared error $\hat{\xi}(n) = e^2(n)$ and updates the coefficient vector with step size μ:

$$\mathbf{w}(n+1) = \mathbf{w}(n) - \frac{\mu}{2} \nabla \hat{\xi}(n) = \mathbf{w}(n) + \mu \mathbf{x}'(n) e(n), \tag{17}$$

where $\mathbf{x}'(n) = s(n) * \mathbf{x}(n)$. Note that the input vector $\mathbf{x}(n)$ must be pre-filtered by $S(z)$; hence the name FXLMS algorithm.

In order to improve convergence of the adaptive algorithm, another LMS-based algorithm, the NFXLMS algorithm is also employed in the work [4]. This algorithm allows us to dynamically adjust the step size μ, in accord with the "filtered" reference input power. In comparison with the FXLMS algorithm, this algorithm is known as being able to provide faster convergence for rapidly fluctuating noise. The weight update formula of NFXLMS algorithm is

$$\mathbf{w}(n+1) = \mathbf{w}(n) + \mu(n) \mathbf{x}'(n) e(n), \tag{18}$$

where $\mu(n)$ is a dynamic step size adjusted according to

$$\mu(n) = \frac{\alpha}{L \hat{P}_x(n)}, \tag{19}$$

where $\hat{P}_x(n)$ is an estimate of the power of filtered reference input $x'(n)$ at time n, and α is a normalized step size satisfying the following criterion

$$0 < \alpha < 2. \tag{20}$$

The power $\hat{P}_x(n)$ can be conveniently estimated using an exponential window that requires only one storage bin:

$$\hat{P}_x(n) = (1-\beta)\hat{P}_x(n-1) + \beta x'^2(n), \tag{21}$$

where β is a smoothing parameter. In order to avoid the problem of dividing by zero when the power estimate $\hat{P}_x(n)$ becomes exceedingly small, a constraint is imposed on the step size

$$\mu(n) = \frac{\alpha}{L \max[\hat{P}_x(n), P_{\min}]}, \tag{22}$$

where $P_{\min}$ is a lower bound on the filtered input power.

3.2 Adaptive Spatially Feedforward Algorithm. An adaptive filter is incorporated into the ANC algorithm to better accommodate uncertainties and perturbations frequently encountered in practical applications. The procedure is considered "hybrid" in a sense since only the FIR part of the controller is made adaptive, while the IIR part remains a structure of comb filter.

To recapitulate, the spatially feedforward controller takes the following form:

$$C_{ideal}(z) = C_{EM}(z) \cdot C_{RP}(z), \tag{23}$$

where

$$C_{EM}(z) = b_0 + \ldots + b_M z^{-M} \tag{24}$$

and

$$C_{RP}(z) = \frac{1}{1 - g z^{-N}} \tag{25}$$

being the FIR part and IIR part, respectively. These expressions are rewritten in z-transform domain.

In lieu of the off-line design described in last section, the transfer function $C_{EM}(z)$ can be realized by a FIR filter and adaptively updated by a modified FXLMS algorithm. The transfer function $C_{RP}(z)$ remains to be a fixed comb filter optimally fit to the repetitive peaks in the frequency response of the spatially feedforward controller. Omitting the argument "(z)," the relevant formulas and weight update rule are summarized as follows:

$$u = C_{EM} * w' \tag{26}$$

$$w' = C_{RP} * w \tag{27}$$

$$C_{EM}(k+1) = C_{EM}(k) - \mu \frac{2eS}{(1 - C_{RP} C_{EM} F)^2} * w' \tag{28}$$

Note, however, that the filter $S/(1 - C_{RP} C_{EM} F)^2$ in the update formula of Eq. (28) contains a term C_{EM} which precludes direct implementation of the update algorithm. To get around the difficulty, a suboptimal but practical approach is adopted. The feedback term in Eq. (27) is thus neglected to obtain a simplified update law for the filter weights

$$C_{EM}(k+1) = C_{EM}(k) - \mu e(k) * (S * w'), \tag{29}$$

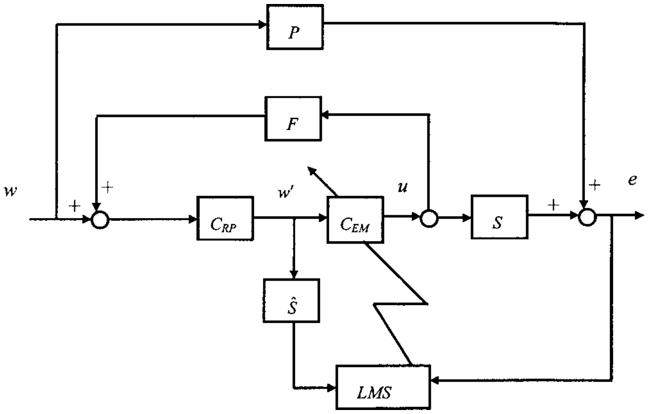

Fig. 4 Block diagram of the adaptive spatially feedforward algorithm

where C_{EM} and S are both realized by FIR filters. Although the instant gradient estimate in the update law seems somewhat biased, the following experiments show that such heuristic approach is effective. The architecture of the entire adaptive spatially feedforward algorithm is summarized in Fig. 4.

As a slight twist of the adaptive algorithm, the convergent speed can be markedly improved by using NFXLMS algorithm which adaptively updates the step size μ according to the power of filtered reference input signal.

4 Experimental Verification

The experimental arrangement is shown in Fig. 5. A wooden duct of length 440 cm and cross-section 25 cm×25 cm is used for verifying the proposed ANC algorithms. The dimensions of the duct and the locations of microphones and loudspeakers are shown in the same figure. There is a 10 cm distance between the primary loudspeaker and the upstream measurement microphone. To minimize acoustic feedback, we made the control loudspeaker facing backward the open end of the duct. The distance between the measurement microphone and the control loudspeaker is 280 cm to ensure causality of the controller. The distance between the control loudspeaker and the downstream performance microphone is 110 cm. A floating-point DSP, TMS320C32, equipped with four 16-bit analog IO channels is utilized to implement the proposed algorithms. The sampling frequency is chosen to be 2 kHz. Considering the cutoff frequency of the duct (approximately 700 Hz) below which exists only plane wave and the poor response of the control speaker below 200 Hz, the control bandwidth is chosen to be 200~600 Hz. In the sequel, experiments are carried out to evaluate the performance of the proposed spatially feedforward algorithms for suppression of the noise in the duct.

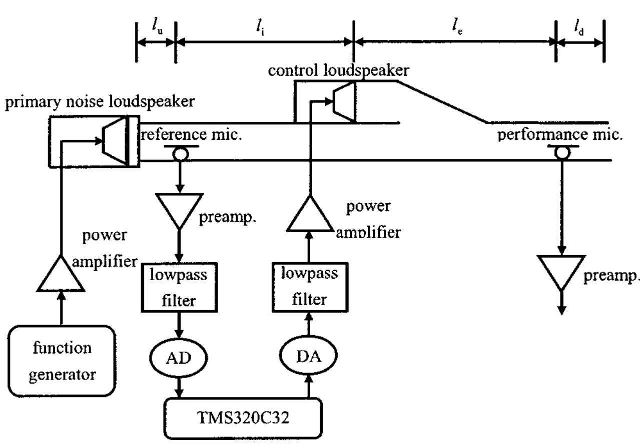

Fig. 5 The experimental setup of a spatially feedforward ANC system

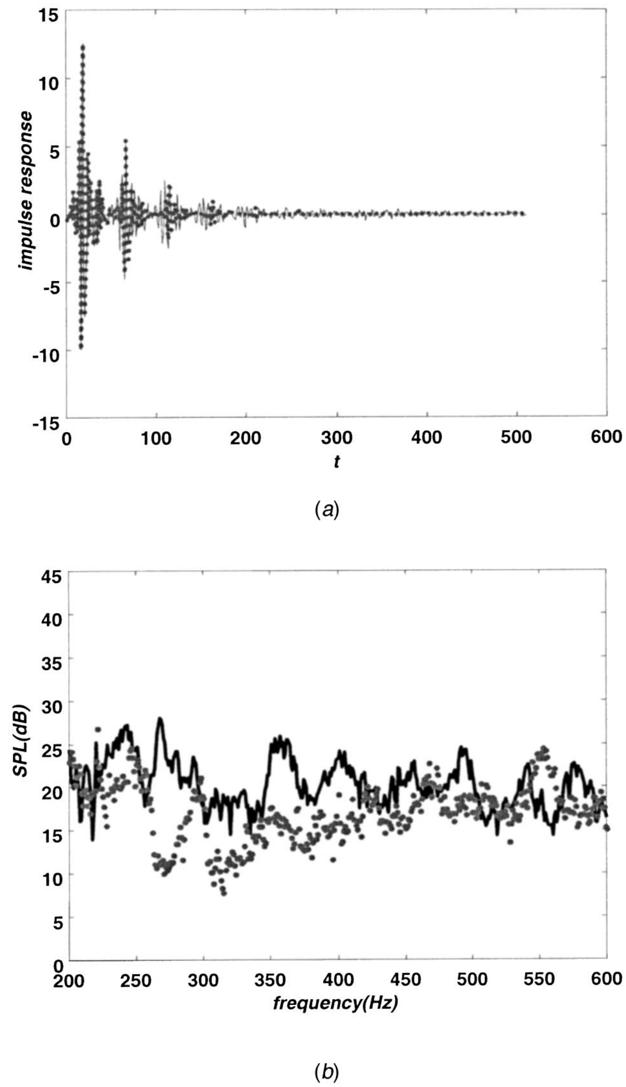

Fig. 6 The fixed spatially feedforward controller (*a*) comparison of the impulse responses between the ideal spatially feedforward controller and the comb filter controller. Ideal controller (—), comb filter controller (----) (*b*) Experimental result in Sound Pressure Level (SPL) of control performance obtained using the fixed spatially feedforward controller. Control off (—), control on (···).

In the first case, the fixed controller is examined. The coefficients of the FIR filter and the comb filter are obtained using the procedure detailed in section 2. In Fig. 6(*a*), good agreement was found by comparing the impulse responses of the fixed comb-filter controller ($N=48, g=0.43$) and the original spatially feedforward controller in Eq. (4). Because the lightly damped dynamics of the repetitive controller has been already represented by a comb filter, the length of the remaining FIR filter has only 48 taps. It can be observed in the experimental results of Fig. 6(*b*), obtained using the fixed controller, broadband attenuation has been achieved (maximum 16.9 dB, band total 3.3 dB). The band total attenuation was the difference in dB between the total sound pressure levels within the band 200~600 Hz, with and without the active control.

In the second case, the adaptive controller using FXLMS algorithm is examined. The frequency response of the spatially feedforward controller calculated using Eq. (4) is shown in Fig. 7(*a*).

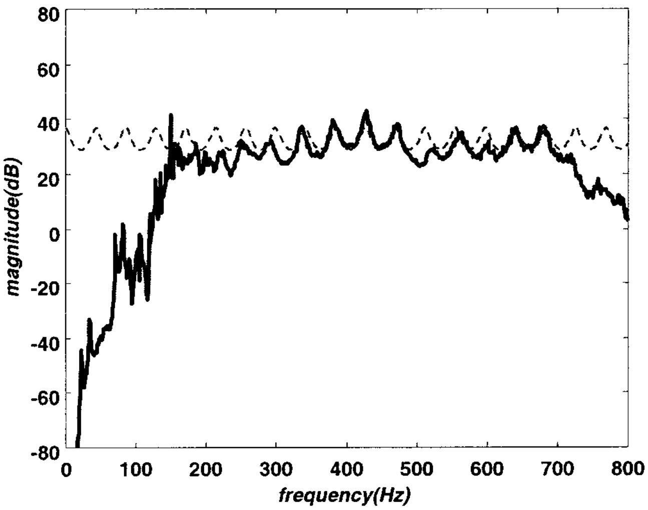

(*a*)

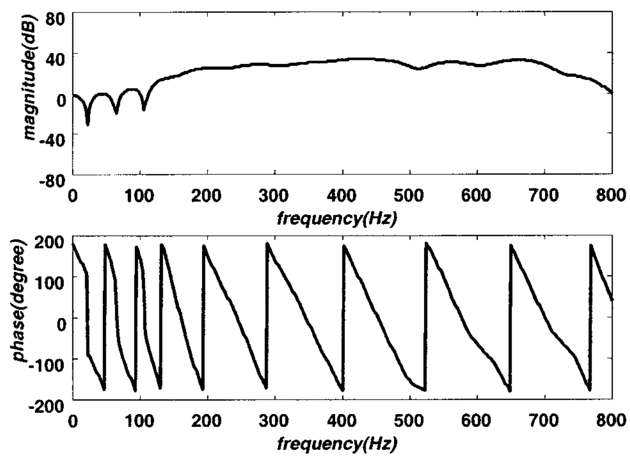

(*b*)

Fig. 7 Design of the adaptive comb filter controller (*a*) The frequency response of the comb filter. Ideal controller (—), comb filter (···) (*b*) The frequency response of the FIR filter.

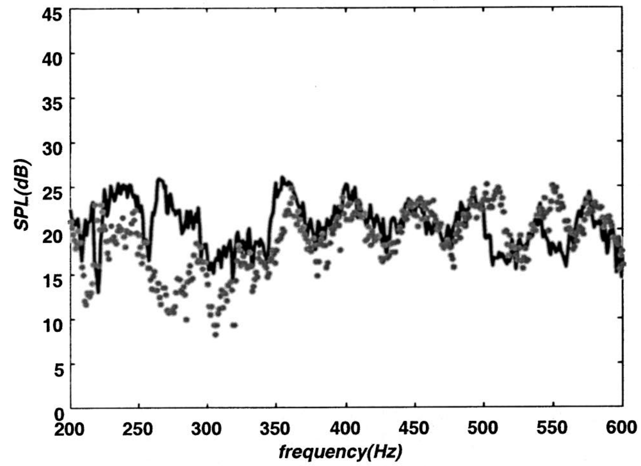

(*a*)

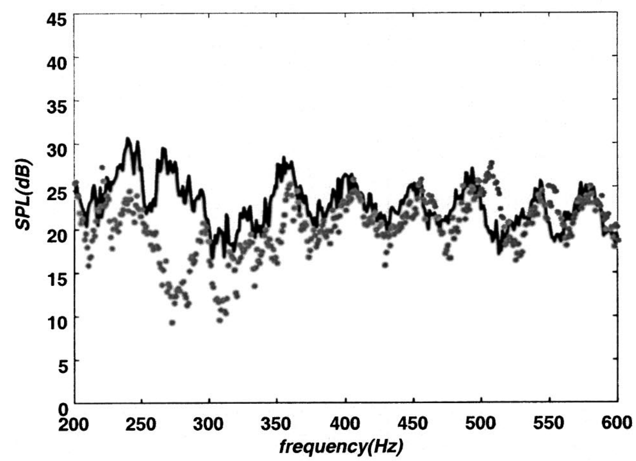

(*b*)

Fig. 8 The experimental results in Sound Pressure Level (SPL) of control performance obtained using adaptive spatially feedforward algorithms (*a*) FXLMS algorithm; (b) NFXLMS algorithm. Control off (—), control on (···).

Then, the repetitive controller is approximated in the control bandwidth by using an IIR damped comb filter. It can be seen in the same figure, the match is acceptable, at least in order, between two frequency responses. It may appear that the match quality between 200 and 300 Hz is not good. However, it turned out that the control performance is not very sensitive to this match quality. The damped comb filter C_{RP} was implemented on the DSP, following the procedure in section 2. On the other hand, the FIR part C_{EM} is adaptively updated by FXLMS algorithm using a reference signal from the output of the comb filter. For reference sake, the frequency response of the FIR filter was also calculated by dividing the spatially feedforward controller with the comb filter, as shown in Fig. 7(*b*). As expected, the frequency response of the FIR filter that is nearly flat, reflecting a relatively simple transducer dynamics. Ideally, the FXLMS algorithm should converge to this fixed FIR filter. Using the FXLMS spatially feedforward algorithm, the experimental result is obtained with a broadband performance (maximum 15 dB, band total 1.8 dB), as shown in Fig. 8(*a*). In addition, the time for convergence is approximately 36 seconds.

In the third case, the adaptive controller using NFXLMS algorithm is examined. In this approach, the step size $\mu(n)$ is adaptively updated with the power of the filtered reference input, the time for convergence has been significantly reduced to approximately 6 seconds, which is a tremendous improvement over the FXLMS algorithm. Using the NFXLMS spatially feedforward algorithm, the experimental result is obtained with a broadband performance (maximum 18 dB, band total 2.7 dB), as shown in Fig. 8(*b*).

From the forgoing results, the proposed spatially feedforward controllers has proved to be effective in suppressing the noise in ducts. The experimental results are summarized in Table 1. It can be observed from the summary, the fixed controller produced slightly better performance (3.3 dB in the band 200~600 Hz) than the other two adaptive methods. In between the adaptive methods, the NFXLMS algorithm not only produced better performance but also faster convergence speed than the FXLMS algorithm. The adaptive controllers appear to be most effective between 200 and 300 Hz. It is suspected that the adaptive algorithms may have an eigenvalue spread problem that is typical in the application of the LMS-based algorithms.

Table 1 Summary of experimental results obtained using the spatially feedforward algorithms

ANC methods	Maximum attenuation	Band total attenuation	Time for convergence
Fixed	16.9 dB	3.3 dB	---
Adaptive FXLMS	15.0 dB	1.8 dB	36 seconds
Adaptive NFXLMS	18.0 dB	2.7 dB	6 seconds

5 Concluding Remarks

In this paper, controllers comprising a nonrecursive filter and a recursive filter have been developed to approximate the ideal spatially feedforward controller for the duct ANC problem. The nonrecursive part represents the dynamics of the transducer, whereas the recursive part is in the form of a comb filter. The parameters of the comb filter are conveniently obtained from the impulse response by using the least-square method. Three approaches are employed to implement the comb filter-based controllers: the fixed algorithm, the FXLMS algorithm, and the NFXLMS algorithm. The advantage of the comb-filter approach lies in primarily the reduced complexity of filter design. The proposed algorithms were implemented using DSP and verified by experiments. All methods have achieved broadband performance, even with the presence of acoustic feedback. While the fixed controller may have achieved slightly better performance than the adaptive methods, the latter approaches could be more useful in applications with system perturbations and uncertainties. Further investigations for practical systems are currently planned to justify this conjecture.

Acknowledgment

The work was supported by the National Science Council in Taiwan, Republic of China, under the project number NSC 89-2212-E-009-007.

References

[1] Elliott, S. J., and Nelson, P. A., 1993, ''Active Noise Control,'' IEEE Signal Process. Mag., **10**, pp. 12–35.
[2] Fontaine, R. F. La., and Shepherd, I. C., 1983, ''An Experimental Study of a Broadband Active Attenuator for Cancellation of Random Noise in Ducts,'' J. Sound Vib., **91**, pp. 351–362.
[3] Swinbanks, M. A., 1973, ''The Active Control of Sound Propagation in Long Ducts,'' J. Sound Vib., **27**, pp. 411–436.
[4] Kuo, S. M., and Morgan, D. R., 1995, *Active Noise Control Systems: Algorithms and DSP Implementations*, John Wiley and Sons, New York.
[5] Bai, M. R., Lin, Y. J., and Wu, J. D., ''Analysis and DSP Implementation of a Broadband Duct ANC System Using Spatially Feedforward Structure,'' ASME J. Vibr. Acoust., (to appear).
[6] Bai, M. R., and Lin, Z., 1998, ''Active Noise Cancellation for a Three-Dimensional Enclosure by Using Multiple-Channel Adaptive Control and H_∞ Control,'' ASME J. Vibr. Acoust., **120**, pp. 958–964.
[7] Hong, J., and Bernstein, D. S., 1998, ''Bode Integral Constraints, Colocation, and Spillover in Active Noise and Vibration Control,'' IEEE Control Syst. Tech., **6**, pp. 111–120.
[8] Munjal, M. L., and Eriksson, L. J., 1988, ''An Analytical, One-Dimensional, Standing-Wave Model of a Linear Active Noise Control System in a Duct,'' J. Acoust. Soc. Am., **84**, pp. 1086–1093.
[9] Tomizuka, M. T. S., and Chew, K. K., 1989, ''Analysis and Synthesis of Discrete-Time Repetitive Controllers,'' ASME J. Dyn. Syst., Meas., Control, **111**, pp. 353–358.
[10] Zolzer, U., 1997, *Digital Audio Signal Processing*, John Wiley and Sons, New York.
[11] Noble, B., 1969, *Applied Linear Algebra*, Prentice Hall, Englewood Cliffs, NJ.